

Measurements and Modeling of Path Loss over Irregular Terrain for Near-Ground and Short-Range Communications

Jiawei Zang* and Xuetian Wang

Abstract—In this paper, radio wave propagation over irregular terrain is investigated in 200–600 MHz (VHF/UHF band). Measured results are compared with different path loss models such as Fresnel knife edge diffraction and uniform theory of diffraction (UTD). It is shown that, for low antenna heights, using a combination of the two-ray path loss model and knife-edge diffraction, great improvement in path loss prediction accuracy is achieved. The derived model is aimed to effectively predict path loss for near-ground and short-range communication applications.

1. INTRODUCTION

The wireless sensor networks (WSN) have shown great potential in military and commercial applications such as military surveillance, environmental observation, and disaster monitoring [1]. Generally, such applications are characterized by low antenna heights with short propagation range. Path loss is a key parameter in wireless communications. The topic of near-ground path loss modeling has been well discussed in [2–9]. Nevertheless, these studies do not offer measurement data or path loss models for irregular terrain that can be used by wireless networks designers. It is necessary to model the path loss over irregular terrain in order to make radio link more reliable. Therefore, radio wave propagation over irregular terrain needs further investigations.

To investigate radio wave propagation over irregular terrain with low antenna heights, measurements are conducted in a hilly region within the 200–600 MHz frequency range. Measured results are compared with several path loss solutions like Fresnel knife-edge diffraction and UTD. This paper introduces a new path loss model, which is a hybrid of the two-ray path loss model and knife-edge diffraction loss model. The proposed model could be used to predict path loss over irregular terrain with non-line-of-sight (NLoS) communications.

2. MEASUREMENT DETAILS AND RESULTS

The selected hilly region mainly consists of soil, low height grass, and small trees. A two-dimensional terrain profile of the measurement site is shown in Fig. 1(a), and a picture of the measurement site is given in Fig. 1(b). The transmitter (Tx) is stationed at the bottom of the hill, and the receiver (Rx) moves on the top of the hill. Different from high mountains with sharp peak, the top of the hill in measurement is a large and fairly flat area, which is usually used for farming. This is also a common scenario in rural area for WSN applications. Near-ground measurements are conducted for Tx-Rx distances of 35–400 m. The line-of sight (LoS) path will be blocked due to the existence of the hill. That means all measurements are performed under NLoS condition. It is clear that the obstructed height tends to increase as the Tx-Rx distance is increased.

Received 28 March 2017, Accepted 15 May 2017, Scheduled 23 May 2017

* Corresponding author: Jiawei Zang (jiaweizang@gmail.com).

The authors are with the School of Information and Electronics, Beijing Institute of Technology, Beijing 100081, China.

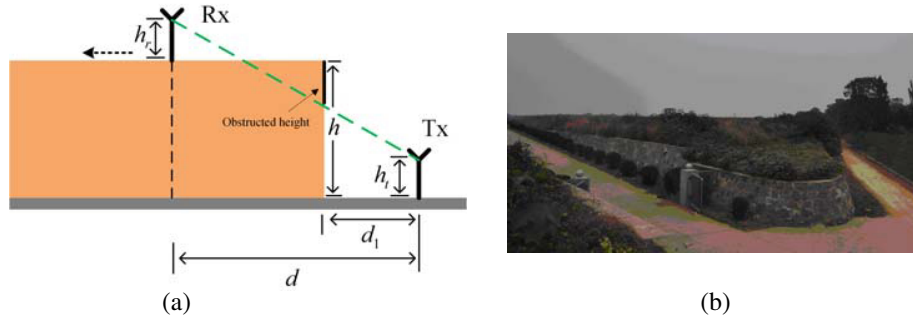


Figure 1. Measurement environment. (a) Two-dimensional geometry. (b) Real picture.

Vertical-polarized omnidirectional dipole antennas are used for both the Tx and Rx. An Agilent E8257 signal generator working in continuous-wave mode is used to feed the transmitting antenna, and the transmit power is fixed at 10 dBm. The measured results are collected by means of an Agilent E4447A spectrum analyzer connected to the receiving antenna through a coaxial cable. The Tx and Rx are fixed at 3.5 m above ground. The parameters of the measurement setup are summarized in Table 1. It should be noted that the distance from the transmitter d_1 should be larger than three wavelengths of the lowest operating frequency for wire antennas to satisfy the far-field conditions. As the frequency range is from 200 to 600 MHz, $d_1 = 8$ m is used. Additionally, this paper mainly concentrates on NLoS communications, to meet NLoS condition, geometry gives the following relationship $d > d_1 (h + h_r - h_t)/(h - h_t)$. Therefore, the Tx-Rx distance starts from 35 m.

Table 1. Parameters of measurement setup.

Transmitting antenna	Omnidirectional radiation, vertical polarization, $h_t = 3.5$ m, Tx-hill distance $d_1 = 8$ m								
Measurement equipment	Agilent E8257 signal generator, coaxial cable, Agilent E4447 spectrum analyzer								
Receiving antenna	Omnidirectional radiation, vertical polarization, $h_r = 3.5$ m								
Hill height	$h = 5$ m								
Frequency (MHz)	200	250	300	350	400	450	500	550	600
Tx-Rx distance d (m)	35	50	70	90	110	130	150	180	210
	240	270	300	350	400				

Since the path loss is the difference value between the transmitting power and the receiving power, the measured path loss PL_m is calculated in the following method based on the receiving power.

$$PL_m(\text{dB}) = P_t - P_r + G_t + G_r - L_{\text{cable}} \quad (1)$$

where P_t is the transmitting power (dBm), P_r the receiving power (dBm), G_t the transmitting antenna gain (dB), G_r the receiving antenna gain (dB), and L_{cable} the total coaxial cable loss of measurements system (dB). Representative results of the measured path loss versus propagation distance at 450 MHz are shown in Fig. 2. The linear regression lines using least mean squares error fitting are also plotted.

It is observed from Fig. 2 that path loss increases exponentially with distance. Traditionally, path loss exponent n , which is related to the radio wave propagation environment, is used to express how fast path loss increases with distance. As reported in [10], different environments exhibit different path

loss exponent values. For example, path loss exponent is 2 for free space, and path loss exponent varies from 2.7 to 3.5 for urban cellular communications. Therefore, it is worthwhile to investigate path loss exponent in irregular terrain with low antenna heights. The derived values of path loss exponent for all frequencies in measurement are given in Table 2. These results show that path loss exponent is large for low antenna heights varying from 3.5 to 4.2. It indicates that the effect of irregular terrain on path loss is noticeable. Therefore, path loss increases more rapidly with distance for low antenna heights.

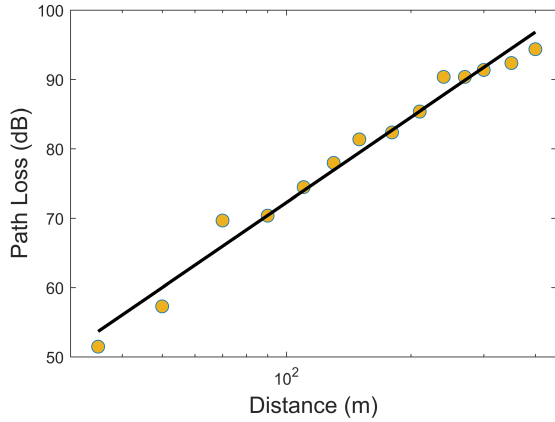


Figure 2. Measured results and linear regression at 450 MHz.

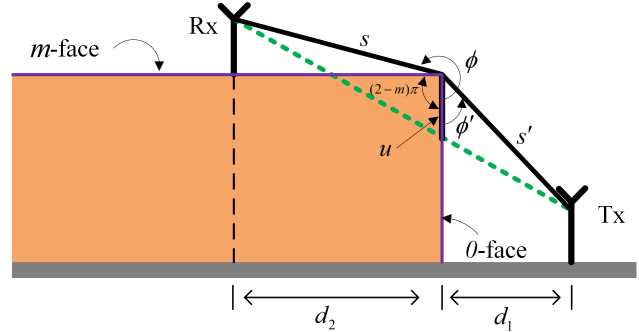


Figure 3. Geometry for wedge diffraction using UTD and knife-edge diffraction.

Table 2. Path loss exponent for each frequency.

Frequency (MHz)	200	250	300	350	400	450	500	550	600
n	4.2	3.9	3.9	4.1	3.6	4.1	3.5	3.8	3.6

3. PATH LOSS MODELING AND DISCUSSIONS

It is conventional to calculate diffraction loss using knife-edge theory and UTD method. The geometry for wedge diffraction using UTD and knife-edge diffraction is shown in Fig. 3. The obstructed height above the LoS path is u , d_2 denotes the distance between Rx and ideal knife edge, the faces of the wedge are labelled as 0-face and m -face, respectively, s' is the distance from Tx to the diffracting wedge, s is the distance from the diffracting wedge to Rx, ϕ' and ϕ are the angles of incidence and diffraction, and the interior angle of the wedge is $(2 - m)\pi$. Clearly, $m = 1.5$ in our cases. From Fig. 3, using knife-edge diffraction theory, the electric field at Rx can be expressed as [11]

$$E_{KE} = E_0 \frac{e^{-jk(d_1+d_2)}}{d_1 + d_2} \left[\frac{1 + j}{2} \int_v^\infty e^{-j(\pi/2)t^2} dt \right] \quad (2)$$

where E_0 is the electric field at Tx, $v = u\sqrt{\frac{2(d_1+d_2)}{\lambda d_1 d_2}}$ the Fresnel-Kirchhoff diffraction parameter under the conditions that $d_1, d_2 \gg u$ and $d_1, d_2 \gg \lambda$, and λ the wavelength. The square bracketed term is known as the complex Fresnel integral. The UTD gives the electric field at Rx as [11, 12]

$$E_{UTD} = E_0 \frac{e^{-jks'}}{s'} D_{\parallel}^{\perp} \sqrt{\frac{s'}{s(s+s')}} e^{-jks} \quad (3)$$

where D_{\parallel}^{\perp} is the diffraction coefficient, which is determined by polarization. For a finitely conducting wedge, D_{\parallel}^{\perp} is given by

$$\begin{aligned} D_{\parallel}^{\perp} = & \frac{-e^{-j\pi/4}}{2m\sqrt{2\pi k}} \times \left\{ \cot\left(\frac{\pi + (\phi - \phi')}{2m}\right) \cdot F(kLa^+(\phi - \phi')) \right. \\ & + \cot\left(\frac{\pi - (\phi - \phi')}{2m}\right) \cdot F(kLa^-(\phi - \phi')) \\ & + R_o^{\perp} \cdot \cot\left(\frac{\pi - (\phi + \phi')}{2m}\right) \cdot F(kLa^-(\phi + \phi')) \\ & \left. + R_n^{\perp} \cdot \cot\left(\frac{\pi + (\phi + \phi')}{2m}\right) \cdot F(kLa^+(\phi + \phi')) \right\} \end{aligned} \quad (4)$$

where

$$F(x) = 2j\sqrt{x}e^{jx} \int_{\sqrt{x}}^{\infty} e^{-j\tau} d\tau \quad (5)$$

and

$$L = \frac{ss'}{s + s'} \quad (6)$$

$$a^{\pm}(\beta) = 2 \cos^2\left(\frac{2m\pi N^{\pm} - \beta}{2}\right) \quad (7)$$

$$N^{\pm} = \text{round}\left(\frac{\beta \pm \pi}{2m\pi}\right) \quad (8)$$

R_o^{\perp} and R_m^{\perp} are the reflection coefficients for perpendicular or parallel polarization for the 0-face, incidence angle ϕ' , and for the m -face, reflection angle $m\pi - \phi$. The typical dielectric constant $\varepsilon_r = 15$ and conductivity $\sigma = 0.005$ S/m [13] is used in this paper to model the finite conductivity wedge surfaces, and hence the reflection coefficients can be calculated.

Finally, path loss based on UTD is given by

$$PL_{UTD} = 20 \log_{10} \left(\frac{\lambda}{4\pi} \frac{|E_{UTD}|}{|E_0|} \right) \quad (9)$$

Similarly, path loss based on knife-edge diffraction theory is given by

$$\begin{aligned} PL_{KE} = & 20 \log_{10} \left(\frac{\lambda}{4\pi} \frac{|E_{KE}|}{|E_0|} \right) \\ = & [-27.55 + 20 \log_{10}(d) + 20 \log_{10}(f)] + 20 \log_{10} \left(\left| \frac{\sqrt{2}}{2} \int_v^{\infty} e^{-j(\pi/2)t^2} dt \right| \right) \end{aligned} \quad (10)$$

where the term within the first square bracket is known as free-space path loss PL_{FR} , with d in meter and f in MHz. Equation (10) shows that the total path loss calculated by classical knife-edge diffraction theory is a combination of free-space path loss and knife-edge diffraction loss $L(v)$. It is well known that free-space path loss model is established under ideal conditions. That means the classical knife-edge approach ignores ground effects, which usually applies to high antenna heights. However, it has been proved that the effect of ground on path loss for low antenna heights is significant. Intuitively, the plane earth path loss model [13] showing a fourth-power law with distance is reasonable to replace the free-space path loss model, which includes the effect of ground. The plane earth path loss model is given as $PL_{Plane} = 40 \log_{10}(d) - 20 \log_{10}(h_t) - 20 \log_{10}(h_r)$. However, the plane earth path loss model is used only when both antennas are on the same ground surface. Therefore, a new variable hill height h should be introduced for situations where transmitting and receiving antennas have different reference levels. In such situations, the calculation of the total path loss is demonstrated in Fig. 4. It is a combination of the two-ray path loss and knife-edge diffraction loss.

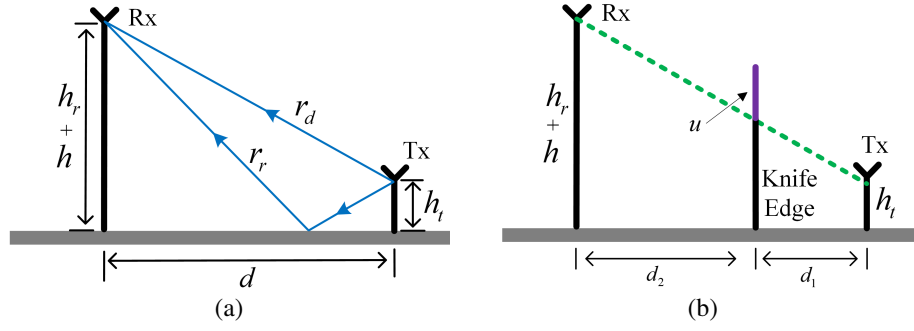


Figure 4. Illustration of the proposed path loss model. (a) Two-ray path loss. (b) Knife-edge diffraction loss.

The two-ray path loss can be obtained by the following approach. From Fig. 4(a), simple geometry gives

$$\begin{cases} r_d = \sqrt{d^2 + (h + h_r - h_t)^2} \\ r_r = \sqrt{d^2 + (h + h_t + h_r)^2} \end{cases} \quad (11)$$

where r_d and r_r indicate the direct and reflected rays. Assuming that the field strength of the direct ray is E_d . Based on two ray theory, the total received field E is

$$\begin{cases} E = E_d [1 + \rho \cdot \exp(-j\Delta\phi)] \\ \Delta r = r_r - r_d \\ \Delta\phi = \frac{2\pi}{\lambda} \Delta r \end{cases} \quad (12)$$

where $\Delta\phi$ is the phase difference between the direct and reflected ray, Δr the path difference, and ρ the ground reflection coefficient. For low antenna height with grazing incidence, $\rho = -1$. Thus, $|E| = 2|E_d| \sin(\Delta\phi/2)$. For isotropic antennas, assuming the transmitting power is P_0 , then the received power P_1 can be expressed by

$$\begin{cases} P_1 = \frac{\lambda^2}{4\pi} S_{AV} \\ S_{AV} = \frac{|E|^2}{120\pi} \\ E_d = \sqrt{\frac{30P_0}{4\pi r_d^2}} \end{cases} \quad (13)$$

where S_{AV} is the average power density at the Rx. For $d \gg h_t, h_r, h$, using Taylor's expansion, we obtain $PL_{Ir} = P_0/P_1 = d^4/(h_t^2(h + h_r^2))$. In logarithmic form, the plane earth path loss model for irregular terrain based on two-ray theory can be written as $PL_{Ir} = 40 \log_{10}(d) - 20 \log_{10}(h_t) - 20 \log_{10}(h_r + h)$. Compared with the traditional plane earth path loss model PL_{Plane} , a new parameter hill height h is added to the path loss model PL_{Ir} . In addition, PL_{Ir} still shows fourth-power law with distance as expected.

From Fig. 4(b), the knife-edge diffraction loss can be easily obtained, which equals $L(v)$ in Equation (10). Then, the total path loss over irregular terrain is

$$PL_{pro} = [40 \log_{10}(d) - 20 \log_{10}(h_t) - 20 \log_{10}(h_r + h)] + 20 \log_{10} \left(\left| \frac{\sqrt{2}}{2} \int_v^\infty e^{-j(\pi/2)t^2} dt \right| \right) \quad (14)$$

Note that the plane earth path loss of irregular terrain only includes antenna heights and hill height and is independent of frequency. In fact, the frequency factor is incorporated in the knife-edge

diffraction loss (parameter v). It is also observed that the plane earth path loss model for irregular terrain shows a fourth-power law with distance rather than the square law of free space path loss of Equation (10). This means a far more rapid increase in path loss with distance, and hence the proposed path loss model appears to be consistent with the measured results.

Other path loss models applicable to the measurement environment are also briefly presented. The Lee model for irregular terrain (obstructive condition), which accounts for additional diffraction loss, is given by [13, 14]

$$PL_{Lee} = PL_0 + \gamma \log_{10}(d) + F_0 + L(v) \quad (15)$$

where PL_0 and γ are derived from empirical data, for example, $PL_0 = 89$ and $\gamma = 43.5$ for rural environment. F_0 is adjustment factor, and $L(v)$ is the knife-edge diffraction loss which can be calculated using the method discussed above. The Blomquist-Ladell model combines the free-space path loss, plane-earth path loss, and knife-edge diffraction loss expressed as [13, 15]

$$PL_{B-L} = PL_{FR} + \left[(PL_{Plane} - PL_{FR})^2 + L(v)^2 \right]^{1/2} \quad (16)$$

The Edwards-Durkin model calculates the total path loss over irregular terrain as [16]

$$PL_{E-D} = \max(PL_{FR}, PL_{Plane}) + L(v) \quad (17)$$

where the larger of the free-space and plane-earth path loss is taken. Note that the knife-edge method is used to calculate diffraction loss for the Lee, Blomquist-Ladell, and Edwards-Durkin models.

Next, we consider which path loss models introduced above best fit irregular terrain with low antenna heights. The traditional free-space-knife-edge path loss model (10), UTD path loss model (9), the proposed path loss model (14), Lee model (15), Blomquist-Ladell model (16), and Edwards-Durkin model (17) are compared with the measured results. The values of mean error and root mean square error (rmse) for these models are summarized in Tables 3 and 4. Figs. 5–7 are illustrative examples showing the comparisons. It is observed that the measured data exhibit small fluctuations. This phenomenon is mainly due to the scattering loss caused by the leaves and grass in measurement environment. We can find that the proposed path loss model predicts a closer fit to the measured results as expected. Compared with the measured data, the Lee model shows large prediction errors with rmse varying from 5.6 to 13.9 dB. This is because the Lee model is an empirical model optimized from collected data for cellular systems. It can be found that the UTD model and the traditional free-space-knife-edge model both show similar predicted results, whereas these two models have slightly poor prediction accuracy with relatively large rmse. It can also be observed that the Blomquist-Ladell model and Edwards-Durkin model show larger rmse than the proposed path loss model. In addition, it is interesting to note that for higher frequencies, the free-space-knife-edge model is likely to overestimate path loss. This findings is consistent with the reported results at 5120 MHz by other investigators in [17, Fig. 7]. This is mainly

Table 3. Mean error (dB) for each path loss model.

Frequency (MHz)	Free-space-knife-edge	UTD	Proposed	Blomquist-Ladell	Edwards-Durkin	Lee
200	-2.2	-2.7	-1.4	-0.1	2.4	-11.4
250	-0.3	-0.7	-1.5	1.5	3.0	-13.6
300	0.2	-0.3	-2.6	1.8	2.6	-11.2
350	0.7	0.2	-3.5	2.3	2.4	-11.3
400	3.7	3.2	-1.6	5.5	4.9	-4.0
450	2.9	2.5	-3.4	4.9	3.8	-10.5
500	5.4	4.9	-1.9	7.6	5.9	-7.9
550	5.1	4.6	-2.9	7.6	5.5	-9.9
600	9.9	9.5	1.1	12.6	10.1	5.1

because the free-space-knife-edge model has a square law with frequency term, which produces a large value at high frequency. In all, the proposed two-ray-knife-edge path loss model is suitable for irregular terrain path loss prediction with low antenna heights.

Table 4. Rmse (dB) for each path loss model.

Frequency (MHz)	Free-space-knife-edge	UTD	Proposed	Blomquist-Ladell	Edwards-Durkin	Lee
200	7.4	7.6	3.9	6.9	5.4	12.0
250	5.3	5.4	2.6	5.9	4.4	13.9
300	5.4	5.5	3.5	6.7	4.0	11.6
350	5.9	5.9	4.2	7.9	4.8	11.7
400	5.8	5.5	3.1	8.6	5.9	5.6
450	6.2	6.1	3.8	9.6	6.1	10.8
500	6.5	6.2	3.4	9.9	6.6	8.9
550	6.8	6.5	3.8	10.7	6.8	10.6
600	10.7	10.3	3.0	14.6	10.8	6.5

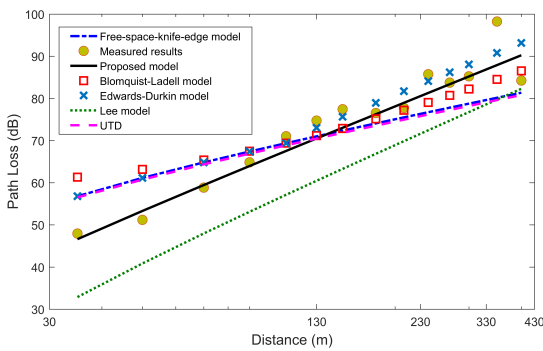


Figure 5. Measured and predicted path loss at 200 MHz.

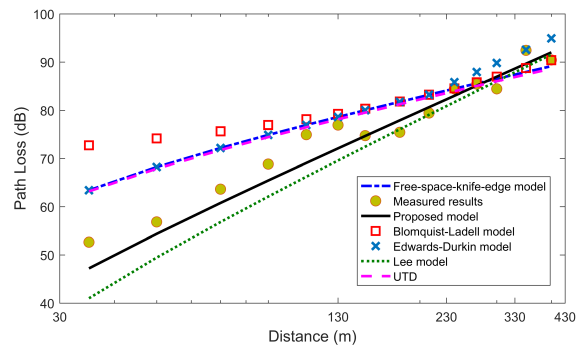


Figure 6. Measured and predicted path loss at 400 MHz.

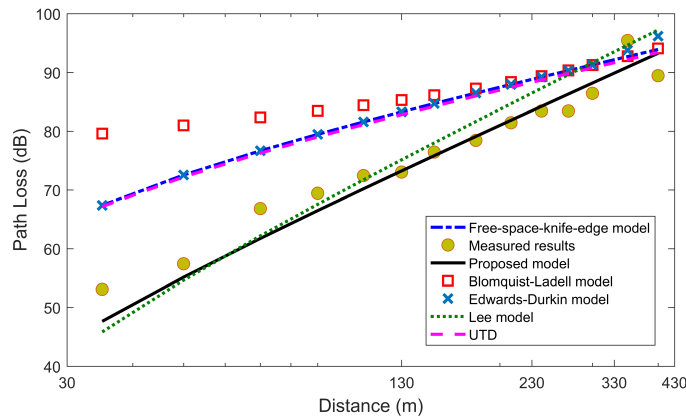


Figure 7. Measured and predicted path loss at 600 MHz.

4. CONCLUSION

In this paper, radio wave propagation over irregular terrain with low antenna heights is investigated. The two-ray-knife-edge model is proposed for path loss prediction. The measured results are compared to various path loss models. It is observed that the proposed model gives a better agreement with measured results, and hence can be adopted to predict path loss over irregular terrain with low antenna heights.

REFERENCES

1. Akyildiz, I. F., W. Su, Y. Sankarasubramaniam, and E. Cavirci, "Wireless sensor networks: a survey," *Computer Networks*, Vol. 38, No. 4, 393–422, 2002.
2. Joshi, G. G., C. B. Dietrich Jr., C. R. Anderson, W. G. Newhall, W. A. Davis, J. Isaacs, and G. Barnett, "Near-ground channel measurements over line-of-sight and forested paths," *IEE Proc. — Microw. Antennas Propag.*, Vol. 152, No. 6, 589–596, 2005.
3. Aslam, M. I. and S. A. Zekavat, "New channel path loss model for near-ground antenna sensor networks," *IET Wirel. Sens. Syst.*, Vol. 2, No. 2, 103–107, 2012.
4. Martinez-Sala, A., J. M. Molina-Garcia-Pardo, E. Egea-Lodpez, J. Vales-Alonso, L. Juan-Llacer, and J. Garcia-Haro, "An accurate radio channel model for wireless sensor networks simulation," *Journal of Communications and Networks*, Vol. 7, No. 4, 401–407, 2005.
5. Hampton, J. R., N. M. Merheb, W. L. Lain, D. E. Paunil, R. M. Shuford, and W. T. Kasch, "Urban propagation measurements for ground based communication in the military UHF band," *IEEE Trans. Antennas Propag.*, Vol. 54, No. 2, 644–654, 2006.
6. Miranda, J., R. Abrishambaf, T. Gomes, P. Gonçalves, J. Cabral, A. Tavares, and J. Monteiro, "Path loss exponent analysis in wireless sensor networks: Experimental evaluation," *2013 11th IEEE International Conference on Industrial Informatics (INDIN)*, 54–58, 2013.
7. AISayyari, A., I. Kostanic, and C. E. Otero, "An empirical path loss model for wireless sensor network deployment in an artificial turf environment," *2014 IEEE 11th International Conference on Networking, Sensing and Control (ICNSC)*, 637–642, 2014.
8. Andrusenko, J., R. L. Miller, J. A. Abrahamson, N. M. M. Emanuelli, R. S. Pattay, and R. M. Shuford, "VHF general urban path loss model for short range ground-to-ground communications," *IEEE Trans. Antennas Propag.*, Vol. 56, No. 10, 3302–3310, 2008.
9. Alsayyari, A., I. Kostanic, and C. E. Otero, "An empirical path loss model for wireless sensor network deployment in a concrete surface environment," *2015 IEEE 16th Annual Wireless and Microwave Technology Conference (WAMICON)*, 1–6, 2015.
10. Rappaport, T., *Wireless Communications: Principles and Practice*, 2nd edition, Prentice Hall PTR, Upper Saddle River, NJ, USA, 2001.
11. Luebbers, R., "Finite conductivity uniform GTD versus knife edge diffraction in prediction of propagation path loss," *IEEE Trans. Antennas Propag.*, Vol. 32, No. 1, 70–76, 1984.
12. Kanatas, A. G., I. D. Kountouris, G. B. Kostaras, and P. Constantinou, "A UTD propagation model in urban microcellular environments," *IEEE Trans. Veh. Technol.*, Vol. 46, No. 1, 185–193, 1997.
13. Parson, J. D., *The Mobile Radio Propagation Channel*, 2nd Edition, Wiley, NY, 2000.
14. Lee, W. C., *Mobile Communications Engineering*, McGraw-Hill, NY, 1982.
15. Blomquist, A. and L. Ladell, "Prediction and calculation of transmission loss in different types of terrain," *NATO-AGARD Conf.*, Publ. CP-144, Res. Inst. Nat. Defense Dept. 3, S-10450, Stockholm 80, 1974.
16. Edwards, R. and J. Durkin, "Computer prediction of service areas for vhf mobile radio networks," *IEEE Proc.* Vol. 116, No. 9, 1493–1500, 1969.
17. Liu, P., D. W. Matolak, B. Ai, and R. Sun, "Path loss modeling for vehicle-to-vehicle communication on a slope," *IEEE Trans. Veh. Technol.*, Vol. 63, No. 6, 2954–2958, 2014.